

## Regular article

# Frontier-orbital analyses of ketene [2 + 2] cycloadditions\*

Shinichi Yamabe<sup>1</sup>, Kayoko Kuwata<sup>1</sup>, Tsutomu Minato<sup>2</sup>

<sup>1</sup> Department of Chemistry, Nara University of Education, Takabatake-cho, Nara 630-8528, Japan

<sup>2</sup> Institute for Natural Science, Nara University, 1500 Misasagi-cho, Nara 631-8502, Japan

Received: 25 June 1998 / Accepted: 28 August 1998 / Published online: 11 November 1998

**Abstract.** Twelve kinds of ketene [2 + 2] cycloadditions have been investigated by ab initio calculations. They are composed of four ketenes (Y–HC=C=O, Y=H, NH<sub>2</sub>, Cl, and CN) and three isoelectronic ketenophiles (ethylene, methylenimine, and formaldehyde). All the transition state geometries obtained here are not different significantly, but the extent of formation of two covalent bonds differs appreciably. The difference is attributable to the degree of the charge transfer interactions. One is the interaction from the  $\pi$  orbital and/or the lone pair orbital of a ketenophile to the LUMO of a ketene (dominant charge transfer, CT1). The other is that from the HOMO of the ketene to the  $\pi^*$  orbital of the ketenophile (second dominant charge transfer, ct1). CT1 contributes to the formation of only one covalent bond, and ct1 does to the formation of the other. This independent function is characteristic of ketene [2 + 2] cycloadditions. They are not concerned with the orbital phase. We also have examined Fukui's postulate that the deformation of particular frontier orbitals causes the reaction progress. The role has been verified both by configuration analyses along the intrinsic reaction coordinate of the ketene-ethylene reaction and by the examination of distortions of frontier-orbital shapes along the low-frequency vibrational modes.

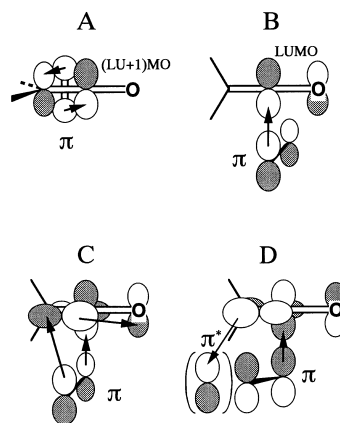
**Key words:** Frontier orbital – [2 + 2] Cycloaddition – Ketene

## 1 Introduction

The molecular orbital is not a physical property and is unrealistic. However, when we admit it as a maxim, the orbital concept can be a general and rational theory to explain and predict organic chemical reactions [1]. There have been various reactivity indices such as Coulson's

free-valence [2] and Wheland's localization energy [3]. However, only Fukui's frontier-orbital theory can be a meaningful and practical tool for organic chemists, because the highest occupied molecular orbital-lowest unoccupied molecular orbital (HOMO-LUMO) interaction is a simple and powerful measure. The frontier-orbital theory is based on the chemical intuition that some active orbitals play a dominant role to determine the chemical reactivity.

The frontier-orbital theory explains most beautifully the Diels-Alder reactions [4]. Bond formations and interchanges can be rationalized by mutual HOMO-LUMO interactions. However, even by the theory, ketene [2 + 2] cycloadditions have not been elucidated satisfactorily. They are called "symmetry-disfavored" reactions according to the Woodward-Hoffmann (W-H) rule [5]. Historically, those reactions have been discussed in various ways, as Scheme 1 shows.



**Scheme 1.** Orbital interactions for ketene [2 + 2] cycloaddition suggested so far

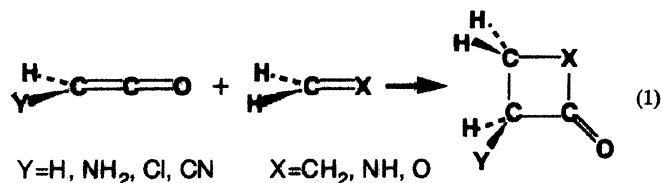
The W-H rule states that the combination of the suprafacial (alkene) and the antarafacial (ketene) approaches leads to the thermally allowed path, [ $\pi 2_s + \pi 2_a$ ] (A in Scheme 1) [5]. In B, the HOMO of alkene  $\rightarrow$  the LUMO of ketene charge-transfer (CT) interaction is depicted. In C, a [2 + 2 + 2] reaction has been speculated [6]. In D, the interactions between the ketene  $\pi_{C=C}$  and

\* Contribution to the Kenichi Fukui Memorial Issue

Correspondence to: S. Yamabe

the alkene  $\pi_{C=C}^*$  orbital and between the former  $\pi_{C=O}^*$  and the latter  $\pi_{C=C}$  orbital are considered [7]. Those ideas are not decisively clear, and the mechanism of ketene [2+2] reactions has not yet been settled. In our communication, a new concept, "dual one-center frontier-orbital interaction", has been put forth [8]. Since the HOMO and LUMO of ketene expand orthogonally, their interactions occur independently. It has been postulated that the two one-center orbital overlap is not concerned with orbital symmetries.

In this work, the concept will be described fully by the use of the 12 [2+2] reactions in Eq. (1).



Their transition states (TSs) will be determined with ab initio calculations. Substituent effects on those cycloadditions will be examined systematically.

Fukui proposed that the deformation of the frontier orbitals caused by the reaction helps the reaction progress. He also put forth the intrinsic reaction coordinate (IRC) [9], and the IRC was combined logically with frontier-orbital theory at an early stage of chemical reaction theory. His postulate will be studied on the basis of the IRC calculation.

The reaction mechanism of ketene [2+2] cycloadditions will be revealed in terms of the frontier-orbital theory.

## 2 Method of calculations

Ab initio calculations were performed by the use of GAUSSIAN 94 program package [10]. TS structures were determined by four methods, RHF/3-21G, MP2(full)/6-31G\*, B3LYP/6-31G\*, and BLYP/6-31+G\*\* [11–14]. Vibrational analyses were carried out with RHF/3-21G, MP2(full)/6-31G\*, and B3LYP/6-31G\* to verify that the obtained geometries are correctly of TSs. IRC calculations [15] were made with RHF/3-21G for parent-ketene reactions to obtain the geometries of their initial stages of the cycloadditions. On these geometries of the ketene-ethylene reaction, configuration analyses [16, 17] were performed to examine the orbital interactions quantitatively. All the calculations were carried out on a CONVEX SPP 1200/XA (Information Processing Center, Nara University of Education) and on a CONVEX SPP 1600/XA (Computer Center, Nara University).

## 3 Results of calculations and discussions

Figure 1 shows the geometries of an early stage and the TS of the ethylene-ketene cycloaddition. At the early stage, ketene and ethylene C=C axes are almost perpendicular. The geometry is similar to that of B in Scheme 1. The ethylene HOMO ( $\pi$ )  $\rightarrow$  ketene LUMO CT interaction is predominant. As the reaction proceeds, the asynchronous character becomes enhanced. That is, one C $\cdots$ C distance is ca. 1.8 Å and the other is ca. 2.4–2.5 Å at the TS. Owing to the former strong C $\cdots$ C

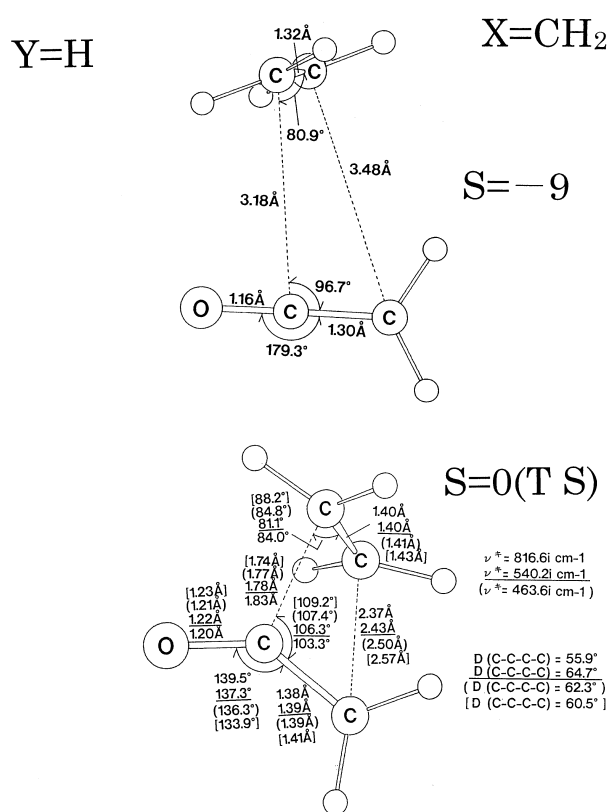


**Fig. 1.** RHF/3-21G geometries of an early stage on the IRC ( $S = -9$  bohr  $\text{amu}^{1/2}$ ) and the transition state (TS,  $S = 0$  bohr  $\text{amu}^{1/2}$ ) of ketene-ethylene [2+2] cycloaddition. TS geometries were also obtained with three other methods, MP2/6-31G\*, (B3LYP/6-31G\*), and [BLYP/6-31+G\*\*]. Empty circles denote hydrogen atoms.  $\nu^{\ddagger}$  stands for the sole imaginary frequency to verify that the obtained geometry is correctly of the TS.  $D$  (C—C—C—C) is the dihedral angle

interaction, the ketene C—O bond has already a carbonyl nature at the TS. The TS geometries calculated by four computational methods are somewhat different. The formation of two new C $\cdots$ C bonds is more asynchronous in the TS geometries obtained by the more reliable methods. The absolute values of the sole imaginary frequencies,  $\nu^{\ddagger}$  values, are smaller by the better methods, which indicates that the more accurate method gives the flat energy maximum to the TS.

The TS geometries of [2+2] cycloadditions between substituted ketenes and ethylene are shown in Fig. 2. Ketenes are by nature electrophilic reagents. An electron-donating substituent, an amino group, is expected to lower the reactivity of ketene-olefin reactions. On the other hand, electron-withdrawing groups, the chloro and cyano groups, will enhance the reactivity. The three TS geometries in Fig. 2 are not different from that in Fig. 1 significantly. However, there are several substituent effects. For  $Y = \text{NH}_2$ , two newly formed C $\cdots$ C bonds are longer than those for  $Y = \text{H}$ . The TS with  $Y = \text{NH}_2$  is early. The C—NH<sub>2</sub> bond length of the TS, 1.38 Å, is shorter than that of the reactant, 1.43 Å. The slight contribution of the C—NH<sub>2</sub> double-bond character is related to the smaller activation energy of  $Y = \text{NH}_2$  than

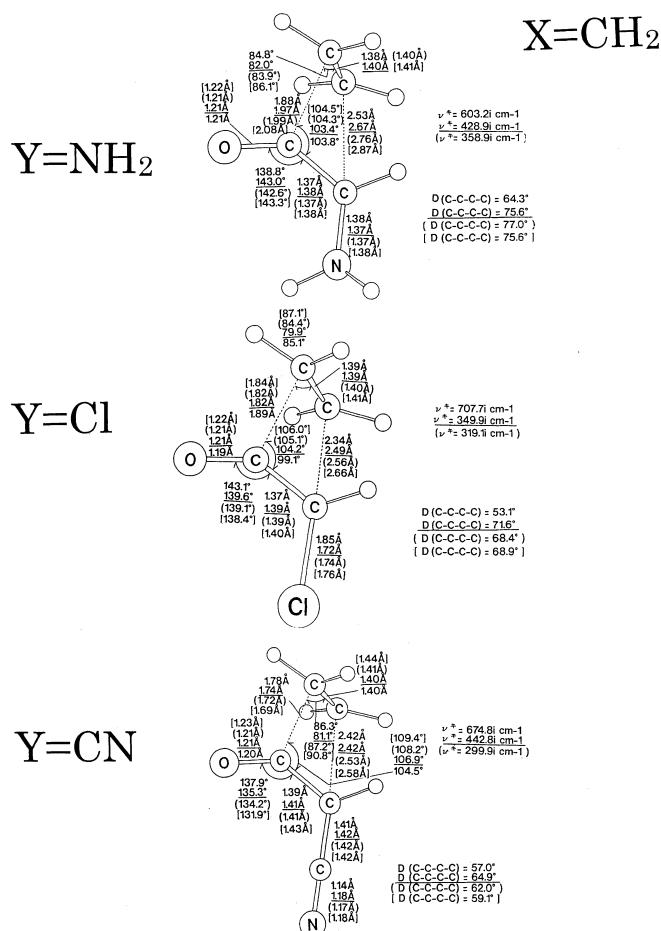


**Fig. 2.** TS geometries of the substituted ketene-ethylene [2+2] cycloadditions

of  $Y=H$  (described later). For  $Y=H$ ,  $NH_2$ ,  $Cl$ , or  $CN$ , the TS geometries are quite asymmetric, and the dominant  $C\cdots C$  bond formation is a common feature. The dependence of TS geometries on computational methods is explained in Fig. 2. While covalent bonds of the higher-level calculations are slightly longer than those of the RHF/3-21G calculation, intermolecular  $C\cdots C$  bonds are relatively sensitive to those methods. At the largest, there is a change of 0.3 Å for  $Y=Cl$ . Noteworthy is the 1.69 Å for  $Y=CN$ , which is extraordinarily, as short a distance as that of the TS. Dihedral angles  $D(\text{C-C-C-C})$  are also susceptible to these methods. The better method tends to give the larger angle.

Figure 3 shows the geometries of an early stage and the TS of the methylenimine-ketene reaction. When the former geometry ( $S = -9 \text{ bohr amu}^{1/2}$ ) is compared with that in Fig. 1, we notice the different inclination of the molecular planes of the two ketenophiles (ethylene and methylenimine). The in-plane lone-pair orbital of methylenimine somewhat participates in the charge donation to the ketene LUMO. If the lone-pair orbital interacts explicitly with the LUMO, an alternative path leading to a zwitterionic intermediate is generated [18–20].

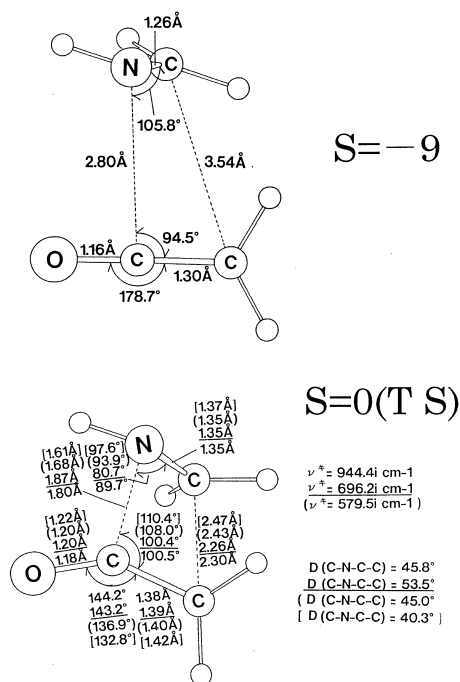
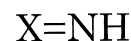
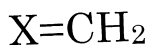


**Fig. 3.** Geometries of an early stage ( $S = -9 \text{ bohr amu}^{1/2}$ ) and TS geometries of the ketene-methylenimine [2+2] cycloaddition. The same notations as in Fig. 1 were used

Since this work is concerned with [2+2] cycloadditions, the path is not discussed although the complete steps have been obtained here with BLYP/6-31+G\*\* (see footnote b of Table 1). The TS geometry in Fig. 3 is similar to that in Fig. 1. That is, the  $\pi$  and  $\pi^*$  MOs of methylenimine interact with ketene orbitals. The  $C\cdots N$  bond is formed predominantly over the  $C\cdots C$  bond.

By the B3LYP/6-31G\* or BLYP/6-31+G\*\* method, the  $C\cdots N$  bond is either 1.68 Å or 1.61 Å, which is shorter than that, 1.80 Å, by RHF/3-21G. This is an appreciable method dependence. Absolute values of the sole imaginary frequencies ( $\nu^\ddagger$  values) also differ for the three methods. The better computational method tends to give the flatter energy maximum.

Substituent effects on TS geometries of the ketene-methylenimine reaction are examined in Fig. 4. Roughly speaking, the  $C\cdots N$  distance is about 1.6 Å and the  $C\cdots C$  one is 2.4 Å by the better methods. For  $Y=NH_2$ , the short  $C-NH_2$  bond in the aminoketene moiety is noteworthy, which is similar to the TS of the ethylene-aminoketene system (Fig. 2). The TS geometry of  $Y=Cl$  is the closest to that of  $Y=H$ . On the other hand, the geometry of  $Y=CN$  is the most different from that of  $Y=H$ . The  $C\cdots N$  distance, 1.5 Å, is very small and is only slightly larger than the covalent-bond distance. The cyanoketene-methylenimine pair can be regarded as a one-center reaction. The dihedral angle,  $D(\text{C-N-C-C})$ , of  $Y=CN$  has the most significant method dependence.

Figure 5 presents the path of the formaldehyde-ketene reaction. At an early stage of the reaction the

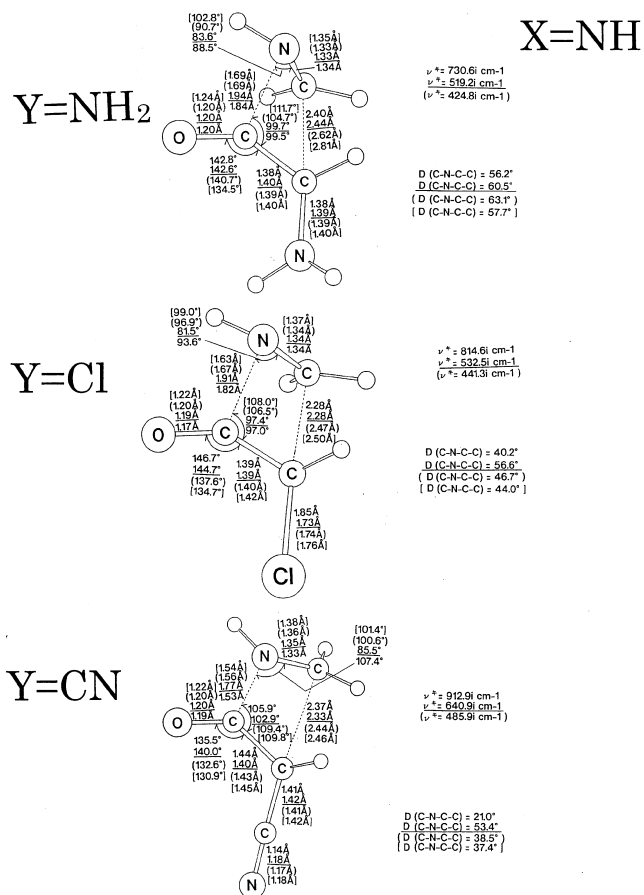


**Fig. 4.** TS geometries of the substituted ketene-methylenimine [2+2] cycloadditions

ketene molecular plane is almost perpendicular to the formaldehyde plane. The lone-pair orbital operates exclusively as an electronic charge donor at the early stage. At the TS, the  $\pi_{C=O}$  MO participates in the  $C \cdots O$  interaction. However, the  $C \cdots O$  distance is large in comparison with the corresponding  $C \cdots C$  (Fig. 1) and  $C \cdots N$  (Fig. 3) ones. On the other hand, the  $C \cdots C$  bond in Fig. 5 is shorter than those in Figs. 1 and 3. The TS shape of the ketene-formaldehyde reaction shows the most “synchronous” bond formation.

Figure 6 shows the TS geometries of the formaldehyde-substituted ketene systems. Substituent effects are overall similar to those in Figs. 2 and 4. For  $Y=CN$ , the  $C \cdots O$  bond is short (1.6–1.8 Å) and the TS geometries are asymmetric. The lone-pair orbital of formaldehyde participates somewhat in the  $C \cdots O$  bond formation. The largest method dependence is found in the dihedral angle,  $D(C-O-C-C)$ , of  $Y=NH_2$ .

Table 1 displays the activation energies ( $E_a$  values) calculated by four methods. The energies calculated by BLYP/6-31+G\*\* are the smallest of the four methods. The RHF/3-21G energies are clearly overestimated. For three ketenophiles ( $X=CH_2$ , NH, or O), the order of the activation energies is  $Y=H > Y=CN > Y=Cl > Y=NH_2$ . The rank of  $E_a(Y=H) > E_a(Y=CN)$  typically reflects Hammett’s rule [21] that the ketene is

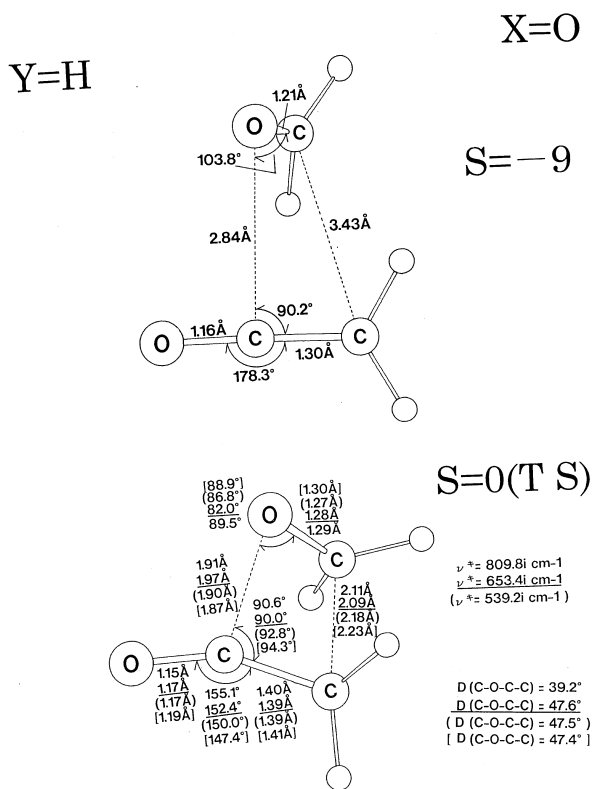
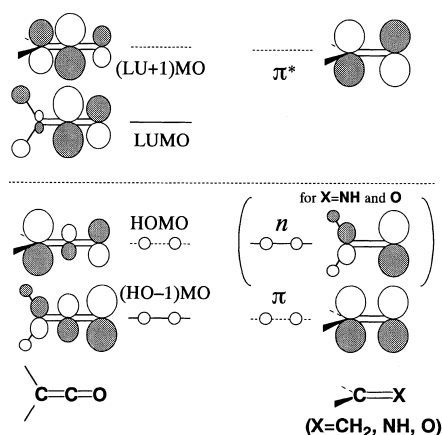


**Fig. 5.** Geometries of an early stage ( $S=-9 \text{ bohr amu}^{1/2}$ ) and the TS of the ketene-formaldehyde cycloaddition. The same notations as in Fig. 1 were used

an electrophile and the ketenophile is a nucleophile. In this respect, the smallest value of  $E_a(Y=NH_2)$  and the order of  $E_a(Y=CN) > E_a(Y=Cl)$  are curious results. This curiosity will be discussed in the next section. The activation energies are compared in three ketenophiles ( $X=CH_2$ , NH, or O) in Table 1. The order  $E_a(X=NH) > E_a(X=CH_2) > E_a(X=O)$  is found. As far as the relation of the nucleophile (ketenophile) and the electrophile (ketene) is concerned, the order appears to be curious. Prior to the calculations, the order  $E_a(X=O) > E_a(X=NH) > E_a(X=CH_2)$  had been expected. Thus, the activation energies in Table 1 demonstrate that the simple donor-acceptor relation does not hold for the ketene [2+2] cycloadditions (a curiosity).

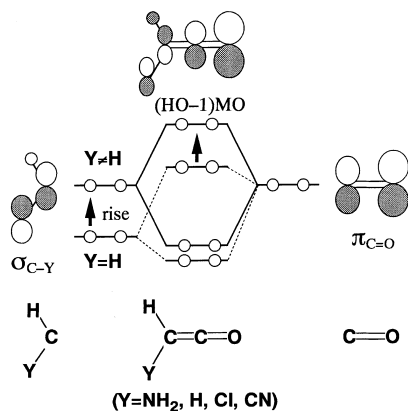
#### 4 Frontier-orbital analyses

In order to solve the curiosity discussed in the previous section, frontier orbitals are now examined. Figure 7 exhibits their orbital energies. The corresponding orbital shapes are drawn in Scheme 2. In the left side of Fig. 7, orbital energies of the ketenes are shown. In the Hammett arrangement, there are two irregularities. One is the smallest energy (0.189 a.u.) of the LUMO of  $Y=Cl$ . The other is the lowest value (−0.471 a.u.) of the (HO−1)MO of  $Y=H$ . Both orbitals are in-plane ones, as Scheme 2 shows.



Scheme 2. Orbital shapes

The irregularity of the (HO-1)MO is explained by the orbital interaction between the  $\sigma_{C-Y}$  orbital of the methylene-type moiety (CHY) and the  $\pi_{C=O}$  orbital of the C=O moiety. The (HO-1)MO is composed of the  $\sigma_{C-Y}$  and  $\pi_{C=O}$  orbitals, as Scheme 3 shows. Since the energy level of the  $\sigma_{C-H}$  orbital is lower substantially than that of the  $\pi_{C=O}$  orbital, the orbital mixing between them is small. Then, the interaction does not raise the energy level of the (HO-1) MO greatly. On the other hand, the energy levels of the  $\sigma_{C-Y}$  orbitals of  $Y=NH_2$ , Cl, or CN are near to that of the  $\pi_{C=O}$  orbital and the  $\sigma_{C-Y} - \pi_{C=O}$  interactions are large. The large interactions raise the energy level of the (HO-1)MO significantly. Thus, the irregularity of the (HO-1)MO level in Fig. 7 is ascribed to the extent of the in-plane  $\sigma_{C-Y} - \pi_{C=O}$  mixing. The smallest extent for  $Y=H$  corresponds to its lowest energy level of the (HO-1)MO.



Scheme 3. Orbital interactions for the formation of the (HO-1)MO

The irregularity of the LUMO energy levels is explained in a similar way. The LUMO is composed of the  $\sigma_{C-Y}^*$  and  $\pi_{C=O}^*$  orbitals. The energy levels of  $\sigma_{C-Y}^*$  orbitals ( $Y=NH_2$ , H, CN) are high relative to that of the  $\pi_{C=O}^*$  orbital and the interactions between them are small. The small interactions do not lower the energy level of the LUMO remarkably. On the other hand, the level of the  $\sigma_{C-Cl}^*$  orbital is close to that of the  $\pi_{C=O}^*$  orbital and the interaction is large. The large interaction lowers the energy level of the LUMO for  $Y=Cl$  substantially. Two irregularities of the energy levels of the

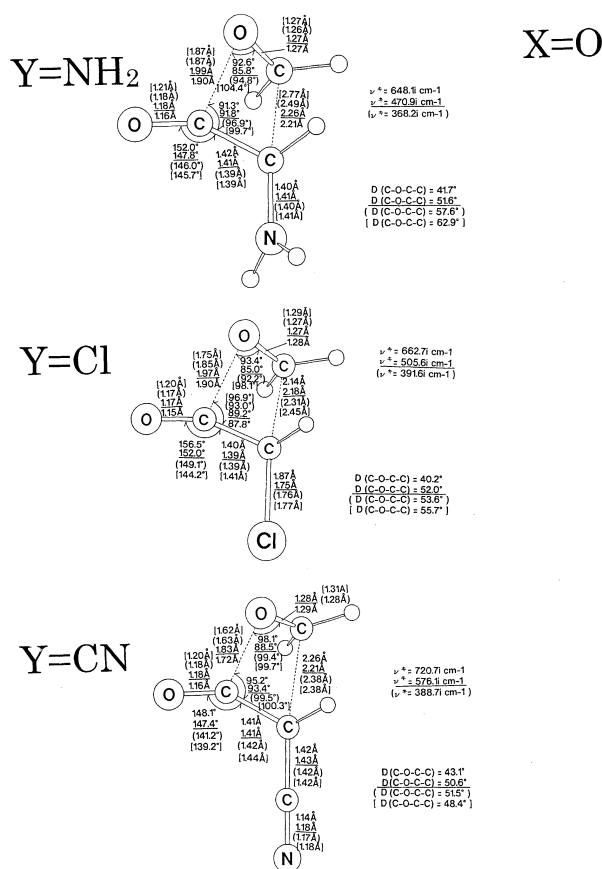


Fig. 6. TS geometries of the substituted ketene-formaldehyde [2 + 2] cycloadditions

in-plane orbitals, (HO-1)MO and LUMO, of ketenes have been explained in terms of the extent of the mixing of fragment orbitals,  $\sigma_{C-Y}$  (or  $\sigma_{C-Y}^*$ ) and  $\pi_{C=O}$  (or  $\pi_{C=O}^*$ ). Table 1 has shown the curious order of  $E_a(Y=CN) > E_a(Y=Cl)$ , which is explicable by the irregularity,  $LUMO(X=CN) > LUMO(X=Cl)$  in Fig. 7.

Energy levels of ketenophiles are examined in the right side of Fig. 7. In formaldehyde, the  $\pi$  orbital has a very low energy ( $-0.440 \text{ a.u.}$ ). Owing to the poor  $\pi$  charge donating strength, the initial geometry ( $S = -9 \text{ bohr amu}^{1/2}$  in Fig. 5) is controlled by the ( $n \rightarrow LUMO$ ) CT interaction. In view of the energy levels of Fig. 7 and the orbital shapes of Scheme 2, it is expected that there are some (not unique) orbital interactions to determine the reactivity of [2 + 2] cycloadditions. Since ketenes are generally electrophiles, their LUMOs are evidently prime frontier orbitals. The LUMO shape is examined in more detail in Fig. 8. The ketene has a cumulative double bond and, accordingly, two small bending vibrational frequencies. The lowest-frequency mode ( $\nu_1 = 531.6 \text{ cm}^{-1}$ ) is the in-plane bending, which changes the LUMO shape (the lower contour map of Fig. 8) as well as lowering the energy ( $0.266 \text{ a.u.} \rightarrow 0.250 \text{ a.u.}$ ). By the in-plane bending, the lobe of the LUMO on the carbonyl carbon is enlarged. That is, the electrophilicity of ketene is enhanced through the lowest-frequency vibration. The charge-transfer and the geometric distortion are coop-

**Table 1.** Activation Energies of [2+2] Cycloadditions of Ketenes to Three Ketenophiles in Kcal/mol<sup>a</sup>

	Method	ketene Y=H	aminoketene Y=NH <sub>2</sub>	chloroketene Y=Cl	cyanoketene Y=CN
Ethylene X=CH <sub>2</sub>	RHF/3-21G	50.8	36.8	39.0	44.2
	MP2/6-31G*	26.9	12.9	14.3	21.6
	B3LYP/6-31G*	26.7	12.6	15.4	20.8
	BLYP/6-31+G**	25.2	10.6	13.6	19.1
Methylenimine X=NH	RHF/3-21G	49.7	38.6	39.5	41.4
	MP2/6-31G*	31.2	18.3	20.9	27.9
	B3LYP/6-31G*	29.5	16.6	20.0	23.2
	BLYP/6-31+G**	28.1 <sup>b</sup>	13.5	18.3	21.7
Formaldehyde X=O	RHF/3-21G	38.8	30.8	30.2	34.9
	MP2/6-31G*	24.9	15.8	16.9	23.8
	B3LYP/6-31G*	23.1	13.0	15.3	20.5
	BLYP/6-31+G**	22.5	9.7	13.5	19.3

<sup>a</sup> By each "Method," TS and reactant geometries were optimized, and their total energies were used to calculate activation energies

<sup>b</sup> There is a two-step route involving a zwitterionic intermediates, which coexists with the [2+2] cycloaddition. The first step is an intermediate formation between methylenimine and ketene with the BLYP/6-31+G\*\* activation energy, 2.3 kcal/mol. The resultant intermediate is by 0.9 kcal/mol stable relative to the reactants. The ring closure of the intermediate to the cycloadduct has an activation energy, 17.6 kcal/mol, relative to the energy of two reactants

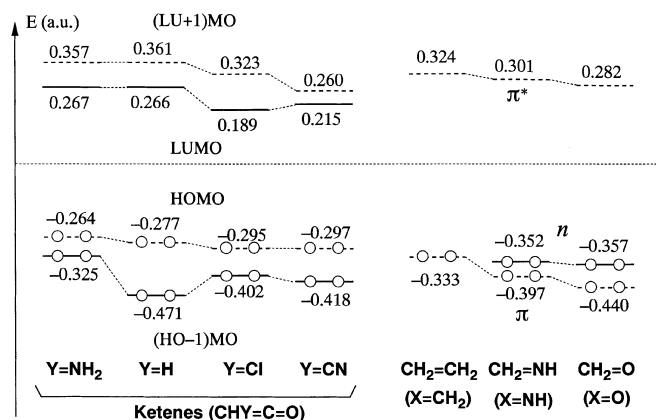
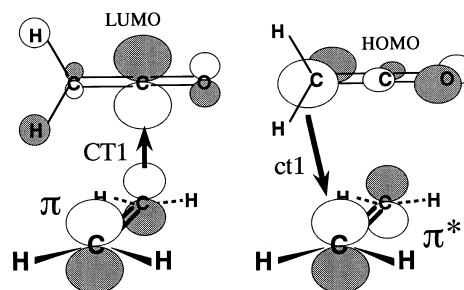


**Fig. 7.** Energy levels (in hartrees) of the frontier orbitals of ketenes, ethylene, methylenimine, and formaldehyde calculated by RHF/STO-3G. The shapes of those orbitals are shown in Scheme 2. In-plane orbitals are shown by *full lines*, and out-of plane ones are by *broken lines*

eratively accelerated along the reaction coordinate. This is one of Fukui's basic ideas [22].

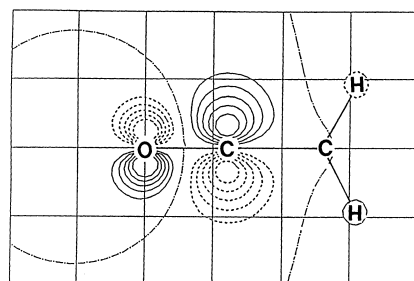
Figure 9 shows the contour map of the (LU+1)MO of ketene. Historically, the (LU+1)MO has been misunderstood as the prime frontier orbital (e.g., A in Scheme 1). A significant shortcoming of the (LU+1)MO is the component of the lobe on both carbonyl oxygen and methylene carbon atoms with a different sign from that of the carbonyl carbon. The electrophilic character on the carbonyl carbon is lessened by the opposite-sign component. Even by the second lowest-frequency vibrational mode ( $\nu_2 = 650.6 \text{ cm}^{-1}$ ), the shortcoming is not relaxed. The opposite-sign lobe is enlarged on the methylene carbon. Thus, the (LU+1)MO cannot be the prime frontier orbital. In Figs. 1, 3, and 5, initial geometries ( $S = -9 \text{ bohr amu}^{1/2}$ ) indicate that the LUMO of ketene is the target for the charge donation.

To verify the frontier-orbital interaction and Fukui's idea, the results of configuration analyses on the ketene-ethylene reaction are shown in Fig. 10. At the early stage ( $S = -9 \text{ bohr amu}^{1/2}$ ), the charge transfer interaction from the  $\pi$  (HOMO) of ethylene to the LUMO of ketene, CT1, is the most important as expected. However, CT1 is not exclusive, and CT2 and ct1 are also contribute appreciably to the progress of the reaction. As the reaction proceeds ( $S = -9 \rightarrow -6 \rightarrow -4 \text{ bohr amu}^{1/2}$ ), CT1 and ct1 grow most among the others. Particular orbital interactions are enhanced by the geometric distortion of the low-frequency vibration. The concentration of the orbital function is called *frontier-orbital theory*. CT1 works for the first C...C bond formation, and ct1 does for the second (late) one. Scheme 4 explains those individual and independent roles. Ketene [2+2] cycloadditions are not concerned with such phase adjustments as in the Diels-Alder reaction. Models A, B, C, and D in Scheme 1 are assessed. The modified D is the correct answer for the ketene [2+2] cycloadditions (Scheme 4). CT1 and ct1 occur simultaneously. Therefore the [2+2] addition can be of a concerted mechanism in spite of the independence.

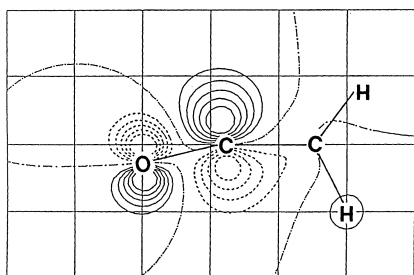


**Scheme 4.** Dual and independent charge-transfer interactions for [2+2] cycloaddition

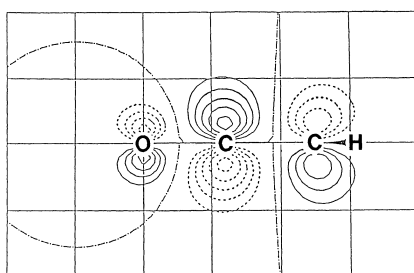
Two curiosities posed in the previous section can be explained by the result of configuration analyses. The first curiosity is the smallest value of  $E_a(\text{Y}=\text{NH}_2)$  in



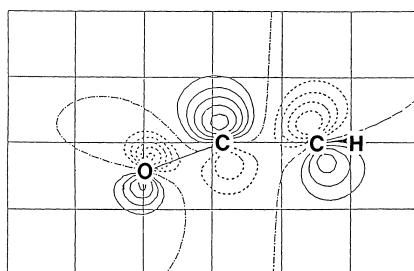
ketene LUMO



**Fig. 8.** Contour curves of the LUMO of ketene. Those of ketene of equilibrium structures and in-plane bent (along the lowest-frequency harmonic vibration) structures are depicted

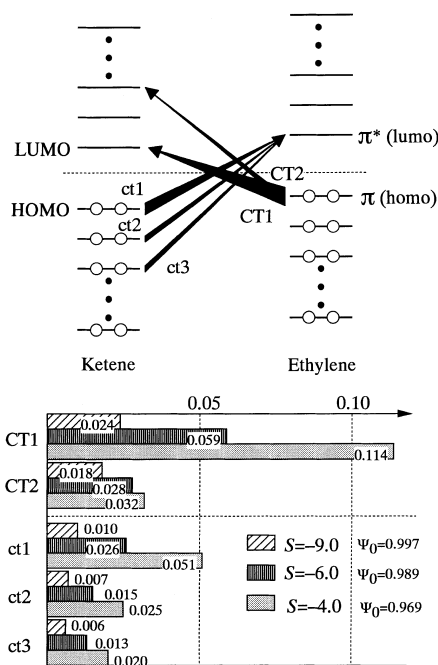


ketene (LU+1)MO



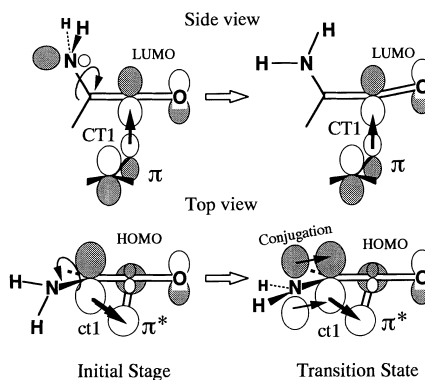
**Fig. 9.** Contour curves of the (LU+1)MO of ketene. Those of ketene of equilibrium structures and out-of-plane bent structures are depicted

Table 1, because the amino group appears to lessen the electrophilicity of ketene. Scheme 5 explains the reason. The lone-pair orbital on the nitrogen atom may strengthen ct1 through conjugation to the ketene HOMO. Since ct1 grows at the late stage of the reaction, the conjugation effectively lowers the activation energy. In fact, the C—NH<sub>2</sub> bond at the TS (Figs. 2, 4, and 6) is somewhat shorter than that of the reactant, aminoketene. The amino conjugation assistance to ct1 is not so



**Fig. 10.** Contributions of dominant configurations except the adiabatical interaction configuration  $\Phi_0$  derived from configuration analysis along the IRC of the ketene-ethylene [2+2] cycloaddition

necessary in the reaction between formaldehyde and aminoketene. Since  $\pi_{\text{C=O}}^*$  is electrophilic enough, ct1 works well even without the assistance. In this regard, the second curiosity,  $E_a(\text{X}=\text{NH}_2) > E_a(\text{X}=\text{CH}_2) > E_a(\text{X}=\text{O})$ , is explained. If it were not for ct1, the order  $E_a(\text{X}=\text{O}) > E_a(\text{X}=\text{NH}) > E_a(\text{X}=\text{CH}_2)$  would be obtained. The highest reactivity of the ketene-formaldehyde reaction is ascribed to the effective ct1. That is, independent and competitive CT1 and ct1 interactions are most typical in the ketene-formaldehyde reaction.



**Scheme 5.** A conjugation effect on enhancement of the HOMO  $\rightarrow$   $\pi^*$  charge-transfer interaction

## 5 Concluding remarks

This work has dealt theoretically with [2+2] cycloadditions between ketenes and three ketenophiles. Three substituents, Y=NH<sub>2</sub>, Cl, or CN, on the ketene are considered. The twelve TS geometries do not differ

significantly. They are composed so that CT1 and ct1 function well. To form two covalent bonds, they work independently. The independent mutual charge-transfer interactions are found also in the ethylene-methylene reaction to form cyclopropane [23]. Basically, ketenes are electrophiles, which states that the LUMO is the prime frontier orbital. Indeed, the initial stage of the [2+2] cycloaddition is governed by the ( $\pi, n \rightarrow$  LUMO) charge-transfer, CT1, but later ( $\text{HOMO} \rightarrow \pi^*$ ), ct1, grows important. In spite of the time lag of their dominant contributions and independence, their synchronous operations make the [2+2] cycloaddition concerted. The apparent anti-Hammett result of activation energies is ascribed to the noticeable contribution of ct1 to stabilizing the reaction system. The role of the frontier orbital becomes more important as the reactant (ketene) is deformed along the low-frequency vibrational mode. The cooperative role of frontier orbitals and facile geometric distortion leads to the IRC. Thus Fukui's postulate has been verified by examination of the LUMO shapes and the results of configuration analyses along the IRC.

**Acknowledgements.** This paper is dedicated to Professor Kenichi Fukui in memory of his career in theoretical chemistry. He deceased on 9 January 1998. He guided the authors S.Y. and T.M. along the path of theoretical chemistry. The authors (S.Y. T.M.) greatly thank Professor Hiroshi Fujimoto for his kind guidance and helpful suggestions during the authors' course of study in Kyoto University.

## References

1. Fukui K, Yonezawa T, Shingu H (1952) *J Chem Phys* 20:722
2. Burkitt FH, Coulson CA, Longuet-Higgins HC (1951) *Trans Faraday Soc* 47:553
3. Wheland GW (1940) *J Am Chem Soc* 62:900
4. Fukui K (1970) *Theory of orientation and stereoselection*. Springer, Berlin Heidelberg New York
5. Woodward RB, Hoffmann R (1970) *The conservation of orbital symmetry*. Verlag Chemie, New York, p 163
6. Zimmerman HE (1977) *Pericyclic reactions*. In: Marchand AP, Lehr RE (eds), vol 1. Academic Press, New York, p 77
7. Ghosez L, O'Donnell MJ (1977) *Pericyclic reactions*. In: Marchand AP, Lehr RE (eds), vol 2. Academic Press, New York, p 85
8. Yamabe S, Minato T, Osamura Y (1993) *J Chem Soc Chem Commun* 450
9. Fukui K (1970) *J Phys Chem* 74:4161
10. Frisch MJ, Trucks GW, Schlegel HB, Gill PMW, Johnson BG, Robb MA, Cheeseman JR, Keith T, Petersson GA, Montgomery JA, Raghavachari K, Al-Laham MA, Zakrzewski VG, Ortiz JV, Foresman JB, Cioslowski J, Stefanov BB, Nanayakkara A, Challacombe M, Peng CY, Ayala PY, Chen W, Wong MW, Andres JL, Replogle ES, Gomperts R, Martin RL, Fox DJ, Binkley JS, Defrees DJ, Baker J, Stewart JP, Head-Gordon M, Gonzalez C, Pople JA (1995) *GAUSSIAN 94*. Pittsburgh, Pa
11. Becke AD (1993) *J Chem Phys* 98:5648
12. Becke AD (1988) *Phys Rev A* 38:3098
13. Lee C, Yang W, Parr RG (1988) *Phys Rev B* 37:785
14. Vosko SH, Wilk L, Nusair M (1980) *Can J Phys* 58:1200
15. Gonzalez C, Schlegel HB (1987) *J Phys Chem* 90:2154
16. Baba H, Suzuki S, Takemura T (1969) *J Chem Phys* 50:2078
17. Fujimoto H, Kato S, Yamabe S, Fukui K (1974) *J Chem Phys* 60:572
18. Assfeld X, Ruiz-Lopez MF, Gonzalez J, Lopez R, Sordo JA, Sordo TL (1994) *J Comput Chem* 15:479
19. Sordo JA, Gonzalez J, Sordo TL (1992) *J Am Chem Soc* 114:6249
20. Cossio FP, Ugalde JM, López X, Lecea B, Palomo C (1993) *J Am Chem Soc* 115:995
21. Hammett LP (1937) *J Am Chem Soc* 59:96
22. Fukui K, Fujimoto H (1969) *Bull Chem Soc Jpn* 42:3399
23. Fujimoto H, S Yamabe S, Fukui K (1972), *Bull Chem Soc Jpn* 45:2424